The Journal of Veterinary Medical Science

FULL PAPER

Virology

Ethyl acetate fraction of flavonoids from *Polygonum hydropiper L.* modulates pseudorabies virus-induced inflammation in RAW264.7 cells via the nuclear factor-kappa B and mitogen-activated protein kinase pathways

Chun-Zhi REN[1,3], Wen-Yue HU[2], Jun-Cheng LI[3], Ying-Hong XIE[1], Ni-Na JIA[1], Jun SHI[1], Ying-Yi WEI[1] and Ting-Jun HU[1]*

[1]College of Animal Science and Technology, Guangxi University, Nanning 530004, PR China
[2]School of Life Sciences & Biotechnology, Shanghai Jiao Tong University, Shanghai, 200030, PR China
[3]Guangxi Agricultural Vocational College, Nanning 530007, PR China

ABSTRACT. Pseudorabies virus (PRV) infection leads to severe inflammatory responses and tissue damage, and many natural herbs exhibit protective effects against viral infection by modulating the inflammatory response. An ethyl acetate fraction of flavonoids from *Polygonum hydropiper L.* (FEA) was prepared through ethanol extraction and ethyl acetate fractional extraction. An inflammatory model was established in RAW264.7 cells with PRV infection to evaluate the anti-inflammatory activity of FEA by measuring cell viability, nitric oxide (NO) production, reactive oxygen species (ROS) release, and mRNA expression of inflammatory factors, inducible nitric oxide synthase (iNOS), and cyclooxygenase-2 (COX-2). Its functional mechanism was investigated by analyzing the phosphorylation and nuclear translocation of key proteins in the nuclear factor-kappa B (NF-κB) and mitogen-activated protein kinase (MAPK) signaling pathways. Our findings indicate that PRV induced inflammatory responses in RAW264.7 cells, and the responses were similar to that in lipopolysaccharide (LPS)-stimulated cells. FEA significantly suppressed NO synthesis and down-regulated both expression and secretion of COX-2, iNOS, and inflammatory cytokines ($P<0.05$ or $P<0.01$). FEA also reduced NF-κB p65 translocation into the nucleus and decreased MAPK phosphorylation, indicating that the NF-κB/MAPK signaling pathway may be closely related to the inflammatory response during viral infection. The findings suggested the potential pharmaceutical application of FEA as a natural product that can treat viral infections due to its ability to mitigate inflammatory responses.

KEY WORDS: ethyl acetate fraction, flavonoids, inflammation, *Polygonum hydropiper L.*, pseudorabies virus

J. Vet. Med. Sci.
82(11): 1781–1792, 2020
doi: 10.1292/jvms.20-0263

Received: 10 May 2020
Accepted: 21 August 2020
Advanced Epub:
1 October 2020

Pseudorabies virus (PRV), a member of the family *Herpesviridae*, infects ruminants, carnivores, rodents, and other mammalian species [15]. The pig is the only natural host of PRV, and PRV infection causes abortion and stillbirth in pregnant sows, recessive infection in adult pigs, and nearly 100% mortality in piglets [25]. With the rapid development of globalization, PRV infection has become widespread worldwide, causing great economic losses to the pig industry [19]. Inflammatory responses accompanied by cytokine release and peroxide production are often observed in PRV-infected animals and are considered as important defenses against viral infection [27, 28, 30, 35]. However, the release of large amounts of inflammatory cytokines and uncontrollable inflammatory responses are triggered in PRV-infected pigs, and these conditions have been speculated to impair and destroy the integrity and function of immune cells. As immune defenses weaken, PRV invades the nervous system of infected animals and causes neurological symptoms such as tremors, ataxia, limb spasm, and intermittent seizures [11, 24, 43]. Currently, no effective drugs for the treatment of PRV infection are available, and preventive measures such as vaccination and breeding management are taken to avoid PRV infection. Unfortunately, due to the high rate of virus mutation, none of the currently available vaccines can provide full protection against PRV infection [4, 48]. Studies found that exogenous antioxidants, such as natural compounds

*Correspondence to: Hu, T.-J.: tingjunhu@126.com

that contain flavonoids, inhibited virus proliferation *in vitro* and alleviated PRV-induced tissue damage by regulating inflammatory responses [30, 51].

Polygonum hydropiper L. (*P. hydropiper L.*) is a traditional Chinese medicinal herb that is widely distributed in the Guangxi and Guizhou provinces of China and is frequently used for treating diarrhea, dyspepsia, itchy skin, rheumatism, and chronic ulcers [13]. Flavonoids are the main effective components in this herb, and ingredients such as rutin, quercetin, hyperoside, quercitrin, galloyl quercitrin, quercitrin, kaempferol, anthraquinones, naphthoquinones, and sesquiterpenoids, have been identified in *P. hydropiper L.* [31]. Modern pharmacological studies report antitumor [39], antiviral [14, 23], antioxidant [5], and anti-inflammatory effects [1, 10] of the flavonoids from *P. hydropiper L.*. Crude extracts of *P. hydropiper L.* have been prepared through water, ethanol, or methanol extraction, but there are limited studies on the purification of the effective ingredients from *P. hydropiper L.* [47]. A crude ethanol extract of *P. hydropiper L.* had been previously purified in our lab via fractional extraction using petroleum ether, chloroform, ethyl acetate, and normal butanol. Higher flavonoid contents were obtained in the ethyl acetate and normal butanol fractions compared to the petroleum ether and chloroform fractions [18, 37]. Excellent antioxidant and antiviral activities were observed in the normal butanol fraction of flavonoids from *P. hydropiper L.* (FNB) in previous studies [2, 20]. However, there are currently no reports on the anti-inflammatory activities of the ethyl acetate fraction of the *P. hydropiper L.* ethanol extract.

We speculate that purified flavonoid extracts of *P. hydropiper L.* may be able to treat viral diseases associated with inflammation. In this study, a model of inflammation was established in RAW264.7 cells infected with PRV. The modulatory effect of the ethyl acetate fractions of the flavonoids from *P. hydropiper L.* on PRV-induced inflammation was evaluated by measuring inflammatory indicators, and the functional mechanism was explored by analyzing the activation of the nuclear factor-kappa B (NF-κB) and mitogen activated protein kinase (MAPK) signaling pathways.

MATERIALS AND METHODS

Materials

Lipopolysaccharide (LPS) and 2,7-dichlorodi-hydrofluorescein diacetate (DCFH-DA) were purchased from Sigma Aldrich, St. Louis, MO, USA. High-glucose Dulbecco's Modified Eagle's Medium (DMEM), fetal bovine serum (FBS), penicillin sodium, and streptomycin were purchased from Gibco, New York, NY, USA. The CCK-8 assay kit and BCA protein assay kit were obtained from Beyotime Institute, Nanjing, China. NO, ROS, and inducible nitric oxide synthase (iNOS) assay kits were obtained from Nanjing Jiancheng, China. ELISA kits for mouse tumor necrosis factor-α (TNF-α), interleukin-1β (IL-1β), interleukin-6 (IL-6), interleukin-10 (IL-10), and cyclooxygenase-2 (COX-2) were purchased from Neobioscience, Shenzhen, China. The RNAiso Plus Kit, PrimeScript® RT reagent Kit, and SYBR® Premix Ex TaqTM II Kit (Perfect Real Time) were purchased from Takara Biotechnology, Dalian, China. Radioimmunoprecipitation assay (RIPA) lysis buffer and the Nuclear and Cytoplasmic Extraction Kit were purchased from CWBIO, Beijing, China. Rabbit antibodies against iNOS, COX-2, IκBα, phosphor-IκBα (p-IκBα), NF-κB p65, p-NF-κB p65, p38, p-p38, JNK, p-JNK, ERK, p-ERK, β-actin, and PCNA, and horseradish peroxidase (HRP)-conjugated goat anti-rabbit IgG were purchased from Cell Signaling Technology, Beverly, MA, USA. ECL reagents were obtained from Merck Millipore, Billerica, MA, USA. Other research grade reagents were supplied by Sinopharm Group Co., Ltd., Shanghai, China, and were used as received.

PK-15 cells and RAW264.7 cells were obtained from the Type Culture Collection of the Chinese Academy of Sciences, Shanghai, China. The pseudorabies virus (PRV, PRV-GXLB-2013 strain), which was isolated from pig tissues, was provided by the Laboratory of Preventive Veterinary Medicine, Guangxi University.

Preparation of ethyl acetate fraction of flavonoids (FEA)

P. hydropiper L. was purchased from Tai Hua Pharmaceutical Co., Ltd., Nanning, China and was identified by Professor Renbin Huang from Guangxi Medical University. The total flavonoids of *P. hydropiper L*. were prepared as previously described [27], and the ethyl acetate fraction was extracted from the obtained total flavonoids. Briefly, 500 g of dried *P. hydropiper L*. was ground into a powder, passed through an 80-mesh screen, and then digested with cellulase and pectinase (0.25% W/V) at 50°C for 1.5 hr. After enzyme inactivation with a sodium carbonate solution, the digested sample was then macerated with ethanol at room temperature for 24 hr. The mixture was filtered with gauze, and the residue was extracted with ethanol again. The filtrate was combined, and the solvent was removed by reduced pressure distillation. A crude extract was obtained with a yield of 52.3%. The crude extract was consecutively extracted using petroleum ether, chloroform, and ethyl acetate, afterwards, the petroleum ether and chloroform fractions were discarded. After removing the solvent through reduced pressure distillation, the ethyl acetate fraction was further purified by XDA-8 macroreticular resin using 75% ethanol as eluent. A yellow powder was obtained with a final yield of 12.1% after removing the solvent, and this was denoted as the ethyl acetate fraction of the flavonoids (FEA) from *P. hydropiper L.*

Quality control of FEA

The total flavonoid content in FEA was determined by ultraviolet spectrophotometry (UV) using rutin as a reference. Specifically, 1 mg FEA was dissolved in 10 ml of ethanol solution (50%, v/v) and transferred into a 50 ml volumetric flask. Next, 10 ml ethanol solution (50%, v/v) and 2 ml sodium nitrite solution (5%, m/v) were added consecutively into the flask. After 6 min incubation at room temperature, 2 ml aluminum nitrate solution (10%, m/v) was added to the mixture, and the solution was incubated at room temperature for another 6 min. Then, 20 ml sodium hydroxide (NaOH) solution (10%, m/v) was added, and the volume of the mixture was adjusted to 50 ml using 50% ethanol (v/v). After thorough mixing, the mixture was allowed to stand

for 15 min. The absorbance was measured at 510 nm using an UVmini-1240 (Shimadzu, Kyoto, Japan). Standard curves were generated using a series of rutin concentrations following the same method, and the total flavonoid content in FEA using rutin as a reference was calculated based on the standard curves.

High performance liquid chromatography (HPLC) was used to determine the contents of rutin, quercitrin, and quercetin in FEA. Analysis was performed on a Waters 2695 separation module (Waters, Milford, MA, USA) fitted with a Waters 2998 photodiode array detector (PDA, wavelength range: 210~400 nm) and an auto sampler. Separation of rutin, quercitrin, and quercetin was achieved by a Waters X Bridge™ C18 HPLC column (4.6 × 250 mm, 5 µm, Waters) using a mobile phase consisting of acetonitrile-0.3% phosphoric acid (27:73, v/v) and an eluent time of 40 min. The sample injection volume was 10 µl, the column temperature was maintained at 30°C, the flow rate was adjusted to 1.0 ml/min, and the detection wavelength was set to 359 nm.

Cell culture and virus analysis

PK-15 cells and RAW264.7 cells were both cultured in completed DMEM containing 10% FBS, 100 U/ml penicillin sodium, and 100 µg/ml streptomycin in a humidified atmosphere at 37°C with 5% CO_2.

After amplifying the virus in PK-15 cells, the infectious titer of PRV was determined using the 50% tissue culture infectious dose ($TCID_{50}$) method. RAW264.7 cells were infected with PRV with a multiplicity of infection (MOI) of 1.1, which did not cause massive death of RAW264.7 cells but resulted in significant inflammatory response.

Quantitative real-time PCR (q-PCR) analysis of PRV gene expression

After inoculation with PRV for 8 hr, q-PCR detection of PRV viral load in the cells was performed as follows: The primers of PRV gE gene (GenBank: MN_443981.1) and mouse housekeeping gene glyceraldehyde phosphate dehydrogenase (GAPDH) (GenBank: NG_007793.4) were designed according to known sequences listed in the GenBank database, PRV gE-qF: 5′-GCTGTACGTGCTCGTGAT-3′, PRV gE-qR: 5′-TCAGCTCCTTGATGACCGTGA-3′. GADPH-qF: 5′-CAATGTGTCCGTCGTGGATCT-3′, GADPH-qR: 5′-TTGAAGTCGCAGGAGACAACC-3′. Total RNA was extracted from the cultures in the 96-well plates after PRV-treatment using TRIzol reagent. Reverse transcription was performed to generate the cDNA using the PrimeScript RT reagent kit. Subsequently, q-PCR was performed in a 96-well format using the SYBR super-mix system on a CFX96™ Real-Time PCR Detection System (Bio-Rad, Hercules, CA, USA) under the following conditions: initial denaturation at 95°C for 30 sec, followed by 36 amplification cycles of 95°C for 5 sec, 60°C for 35 sec, and a final extension at 72°C for 10 min. After the reaction, the fusion curve was analyzed to identify the specificity of PCR products, and the relative values for the gene levels were calculated using the $2^{-\Delta\Delta Cq}$ method.

Infection of RAW264.7 cells with PRV

Seven groups were set up for all the cell culture experiments, namely, the control group, LPS group, PRV group, rutin group (positive control drug), FEA25 group, FEA50 group, and FEA100 group. RAW264.7 cells were seeded in 96-well (2×10^4 cells/well), 24-well (5×10^5 cells/well), and 6-well (5×10^6 cells/well) plates for analysis of cell viability, NO and ROS generation, secretion and mRNA expression of key inflammatory cytokines, and production or phosphorylation of key proteins in the NF-κB signaling pathway. After overnight culture, the supernatant was discarded, and the cells were administered PRV at a MOI of 1.1. Cells in the LPS groups were stimulated with LPS at a concentration of 1.0 µg/ml, whereas DMEM was used in the control group. After 1.5 hr, the supernatant was removed, and the cells were washed thrice with phosphate-buffered saline (PBS, 10 mM, pH7.2). Cells in the control, PRV, and LPS groups were cultured with complete DMEM, while the cells in the rutin and FEA groups were treated with rutin (40 µg/ml) or FEA (25, 50 or 100 µg/ml), respectively. The cells were further cultured for 8 hr before performing subsequent analyses.

Cell viability test

Primarily, the cytotoxicity of FEA on the cells was measured. RAW264.7 cells were seeded in 96-well plates at a concentration of 2×10^4 cells/well and were cultured overnight. The cells were then treated with a series of concentrations of FEA for 8 hr. The supernatant was removed, and cell viability was determined using a CCK-8 assay kit following the manufacturer's instructions. Briefly, the supernatant was removed, and CCK-8 diluted in DMEM was subsequently added into the wells. After 1 hr of incubation, optical density was measured at 450 nm on a multifunctional microplate spectrophotometer (Tecan, Zurich, Switzerland). Cell viability was calculated as a percentage of that of the control group.

In addition, cell viability after PRV and FEA treatment was also determined using the CCK-8 assay.

NO determination

After the treatments, the supernatants were collected from the 24-well plates and were then centrifuged for 15 min at 4,000 rpm. NO concentration was determined using a NO assay kit (Microwell plate method) according to the manufacturer's instructions. Optical densities were measured at 540 nm.

ROS determination

ROS production was measured using an ROS assay kit. After the cells in the 24-well plates were treated as described above, 10 µM of the DCFH-DA probe was added and the cells were incubated at 37°C for 30 min. After washing thrice, 1 ml PBS was added to each well, and 0.2 ml of the cell suspension was transferred to a 96-well black-walled plate. Fluorescence was measured at an excitation wavelength of 488 nm and an emission wavelength of 520 nm.

Determination of inflammatory cytokines and activities of COX-2 and iNOS

Supernatants obtained from the 24-well plates were used to determine the levels of TNF-α, IL-1β, IL-6, IL-10, and COX-2 using ELISA kits. The cell supernatant was prepared through supercentrifugation and sonication, and the iNOS activity in the supernatants was quantified using an iNOS typed assay kit (colorimetric method) based on the manufacturer's instructions.

qPCR analysis of gene expression

The total mRNA was extracted and reverse transcribed into cDNA, as described above. Quantitative real time PCR was performed using the cDNA as a template to measure gene expression in a 20 µl reaction system under the following conditions: initial denaturation at 95°C for 30 sec, followed by 35 amplification cycles of 95°C for 10 sec, 55°C for 10 sec, and 72°C for 15 sec, and a final extension step at 72°C for 10 min. β-actin was used as the internal reference gene. The relative values for mRNA levels were calculated using the $2^{-\Delta\Delta Cq}$ method and are presented as the fold change relative to the internal reference gene β-actin. The primer sequences used are as follows: TNF-α, forward primer, 5′-GCAGGTCTACTTTGGAGTCA-3′, reverse primer, 5′-ACATTCGAGGCTCCAGTGAA-3′; IL-1β, forward primer, 5′-GAAATGCCACCTTTTGACAGTG-3′, reverse primer, 5′-TGGATGCTCTCAGGACAG-3′; IL-6, forward primer, 5′-GAGGATACCACTCCCAACAGACC-3′, reverse primer, 5′-AAGTGCATCATCGTTGTTCATACA-3′; IL-10, forward primer, 5′- CGGGAAGACAATAACTG-3′, reverse primer, 5′- CATTTCCGATAAGGCTTGG-3′; monocyte chemotactic protein-1 (MCP-1), forward primer, 5′-CCACTCACCTGCTGCTACTCAT-3′, reverse primer, 5′-TGGTGATCCTCTTGTAGCTCTCC-3′; COX-2, forward primer, 5′-AATGAGTACCGCAAACGCTTCT-3′, reverse primer, 5′-TTCTGCAGCCATTTCCTTCTC-3′; iNOS forward primer, 5′-TTTGCTTCCATGCTAATGCGAAAG-3′reverse primer, 5′-GCTCTGTTGAGGTCTAAAGGCTCCG-3′; NF-κB P65, forward primer, 5′-GACCTGGAGCAAGCCATTAG-3′, reverse primer, 5′-CACTGTCACCTGGAAGCAGA-3′; β-actin, forward primer, 5′-TTCCTTCTTGGGTATGGAAT-3′, reverse primer, 5′-GAGCAATGATCTTGATCTTC-3′.

Western blot determination of protein expression and phosphorylation

Cells cultured in the 6-well plates were collected, and the total proteins were extracted using RIPA lysis buffer supplemented with a cocktail of protease inhibitors and phosphatase inhibitors. The cytoplasmic and nuclear protein fractions were obtained using a commercial Nuclear and Cytoplasmic Extraction Kit following the manufacturer's instructions. Protein concentration was determined using a BCA protein assay kit. The proteins (50 µg in total content) were first separated on SDS-PAGE gels, and the proteins in the gels were transferred onto PVDF membranes. The membranes were blocked with bovine serum albumin (BSA, 5% w/v) at room temperature for 1 hr and were then incubated with the appropriate diluted primary rabbit antibodies against iNOS, COX-2, IκBα, p-IκBα, NF-κB p65, p-NF-κB p65, p38, p-p38, JNK, p-JNK, ERK, p-ERK, β-actin, or PCNA at 4°C overnight. After washing four times with Tris Buffered Saline Tween (TBST) buffer, the membranes were incubated with HRP-conjugated goat anti-rabbit IgG at 37°C for 1.5 hr. The immunoreactive bands were visualized with ECL reagents on a Bio-Rad chemiluminescence imaging system. ImageJ software was used for quantitative analysis of the protein bands.

Statistical analysis

The data are presented as mean ± standard deviation (SD). Statistical analysis was performed using one-way analysis of variance (ANOVA) followed by the Bonferroni's *post-hoc* test on SPSS 23.0. $P<0.05$ was considered statistically significant, and $P<0.01$ was considered as extremely significant.

RESULTS

Preparation and quality control of FEA

The yield of the crude extract obtained from ethanol extraction was 52.3%. FEA was obtained as a yellow powder substance at a yield of 12.1% through petroleum ether, chloroform, and ethyl acetate extraction. The total flavonoid contents in the extract was quantitatively determined to be 56.8% through the colorimetric method using rutin as the standard. The characteristic peaks of rutin, quercitrin, and quercetin were clearly distinguished from the other constituents using HPLC, showing retention times of 7.92 min, 11.91 min, and 26.53 min, respectively. Based on the standard curves prepared by measuring a series of concentrations of the rutin, quercitrin, and quercetin standards, the contents of these three constituents in FEA were calculated to be 281.97 mg/g, 160.98 mg/g, and 83.31 mg/g, respectively, accounting for a total of 52.63% of FEA (Fig. 1).

Analysis of infection in PK-15 and RAW264.7 cells

Figure 2A and 2B shows that PRV mRNA were highly expressed in both PRV-induced PK-15 cells and RAW264.7 cells, and the above-mentioned changes were consistent with those in PRV positive control group, indicating that the virus had successfully infected the PK-15 cells and RAW264.7 cells.

Cytotoxicity of FEA and its effect on PRV-induced cell viability

Safety issues are of the greatest concern during the very early stage of drug development. Figure 3A shows that no significant difference was observed in RAW264.7 cells treated with FEA at concentrations lower than 200 µg/ml; however, high concentrations of FEA (≥400 µg/ml) caused a significant decrease in cell viability ($P<0.05$). Notably, FEA at concentrations of 50 and 100 µg/ml slightly stimulated the proliferation of RAW264.7 cells, which showed higher viability compared to the control

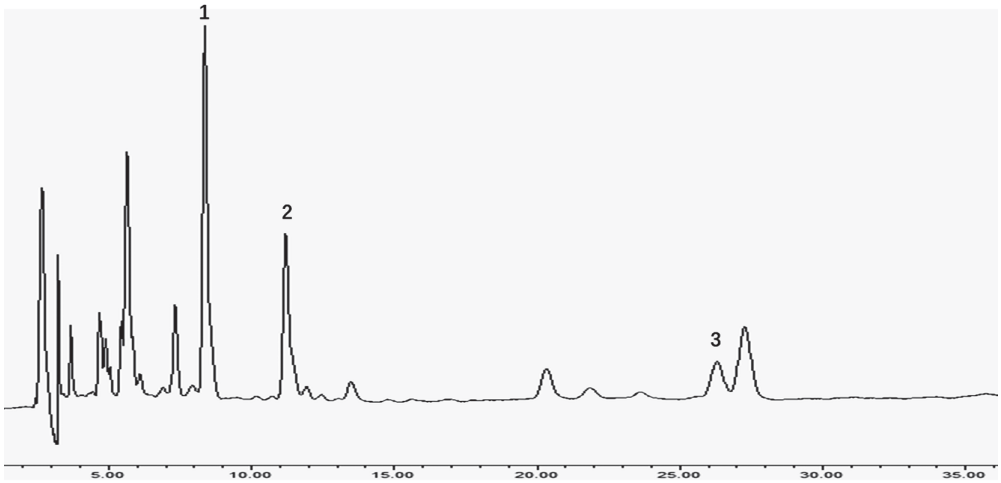

Fig. 1. High performance liquid chromatography analysis of ethyl acetate fraction of flavonoids from *Polygonum hydropiper L.* 1: rutin 2: quercitrin 3: quercetin.

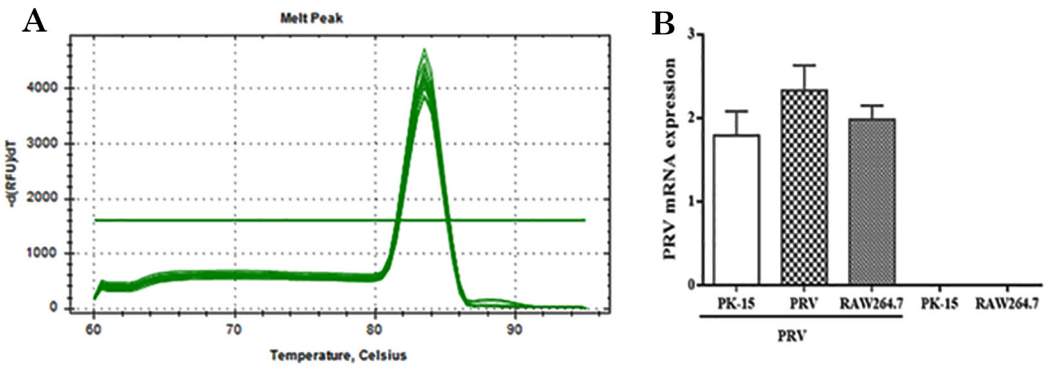

Fig. 2. Analysis of Pseudorabies virus infection in PK-15 cells and RAW264.7 cells. A: Dissolution curves of Pseudorabies virus (PRV) gene; B: PRV mRNA expression in PK-15 and RAW264.7 cells.

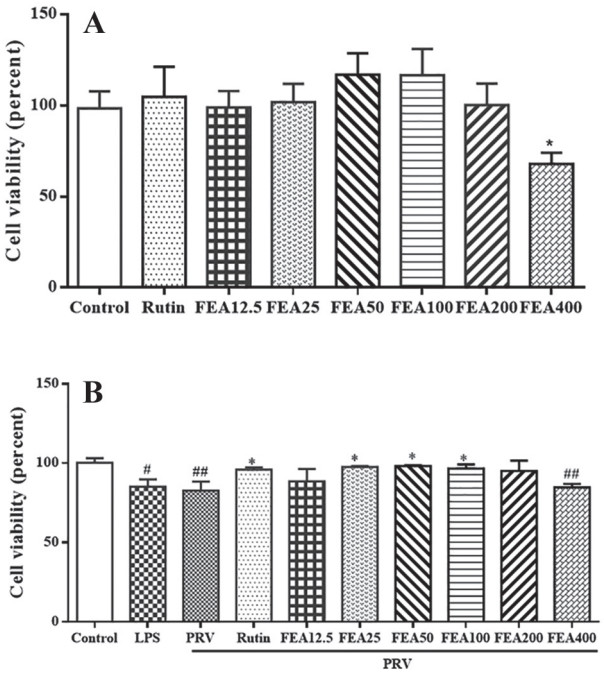

Fig. 3. Effects of ethyl acetate fraction of flavonoids from *Polygonum hydropiper L.* treatment on cell viability. Cell viabilities were determined using a CCK-8 assay. A: Cell viabilities in RAW264.7 cells treated with ethyl acetate fraction of flavonoids (FEA). B: Cell viabilities in RAW264.7 cells treated with FEA after Pseudorabies virus (PRV) infection. FEA12.5-400 means that the dose of FEA used was 12.5 μg/ml, 25 μg/ml, 50 μg/ml, 100 μg/ml, 200 μg/ml, and 400 μg/ml, respectively. # or ## means comparison between the control group and all other groups (lipopolysaccharide (LPS) group, PRV group, rutin group, and FEA groups) (P<0.05, or P<0.01). * or ** only means comparison between PRV group and treatment groups (rutin group and FEA groups) (P<0.05, or P<0.01).

RAW264.7 cells.

Figure 3B shows the viability of RAW264.7 cells after PRV infection and FEA treatment. PRV infection significantly decreased the viability of RAW264.7 cells ($P<0.01$), while both rutin and FEA treatments protected the RAW264.7 cells from a PRV-induced decrease in cell viability. Among the tested concentrations, 25, 50 and 100 µg/ml FEA exhibited the strongest protective effects, leading to significantly increased cell viability compared to those induced by PRV alone ($P<0.05$ or $P<0.01$). Therefore, FEA was used at concentrations between 25 and 100 µg/ml in subsequent experiments.

Effect of FEA on NO and ROS generation

As Fig. 4A and 4B shows, NO and ROS levels were dramatically increased in RAW264.7 cells after PRV infection ($P<0.01$), which showed a more potent stimulus effect than LPS; however, FEA at concentrations of 50 and 100 µg/ml obviously reduced NO generation after 8 hr of incubation ($P<0.05$ or $P<0.01$). At all tested concentrations, 40 µg/ml rutin and FEA exhibited strong, dose-dependent inhibitory effects on ROS generation in PRV-infected cells ($P<0.01$).

Effect of FEA on inflammatory cytokine secretion and on COX-2 and iNOS activities

Secretion of inflammatory cytokines, including TNF-α, IL-1β, IL-6, and IL-10, was significantly increased after incubation with PRV ($P<0.05$ or $P<0.01$), and this effect was similar to or stronger than that of LPS (Fig. 4C–F). Both rutin and FEA treatments reduced the inflammatory cytokine contents in the culture supernatants of the PRV-induced RAW264.7 cells. Secreted levels of TNF-α, IL-1β, IL-6, and IL-10 in all the treated groups were more evident than those in the PRV group ($P<0.05$ or $P<0.01$). Among the tested concentrations, 25 µg/ml FEA exhibited the strongest regulatory effect on TNF-α, IL-1β, and IL-6, while higher concentrations of FEA showed a stronger effect on IL-10. PRV infection caused extremely high COX-2 and iNOS activities in the supernatant ($P<0.01$), and treatment of the cells with 40 µg/ml rutin and FEA at all tested concentrations significantly decreased COX-2 and iNOS secretion from the PRV-induced cells ($P<0.01$) (Fig. 4G and 4H).

Effect of FEA on gene expression

Expression of inflammatory cytokine genes and genes associated with inflammation were analyzed through q-PCR (Fig. 5). A marked up-regulation of the mRNA expression of genes encoding inflammatory cytokines including TNF-α, IL-1β, IL-6, IL-10, and MCP-1 was observed in the PRV-induced RAW264.7 cells ($P<0.05$ or $P<0.01$), and these results were similar to those observed after LPS stimulation. After FEA treatment at different concentrations, the expressions of these genes were significantly inhibited; however, after treatment with rutin, there were only significant differences in the gene expressions of IL-1β and IL-6 when compared with PRV group ($P<0.05$ or $P<0.01$). In addition, a similar phenomenon was observed in the mRNA levels of COX-2 and iNOS; that is, these levels were up-regulated in PRV-induced cells but were down-regulated in rutin- or FEA-treated cells. Among the tested concentrations, 25 µg/ml FEA exhibited the strongest regulatory effect on the mRNA expressions of IL-1β and IL-6 ($P<0.01$), 50 µg/ml FEA remarkably inhibited the mRNA expressions of TNF-α and MCP-1, and 100 µg/ml FEA showed the best inhibitory effect on the mRNA expressions of IL-10, COX-2, and iNOS ($P<0.01$). Regarding NF-κB p65, which is a key protein in the NF-κB signaling pathway, significantly higher mRNA levels were observed in the PRV-induced cells than in the control cells ($P<0.01$). Expression of this gene was inhibited by rutin and FEA treatment, and 50 µg/ml FEA had the strongest inhibitory effect on the PRV-induced expression of NF-κB P65 ($P<0.01$). These results were consistent with the levels of inflammatory cytokines in the culture supernatants shown in Fig. 4.

Effect of FEA on COX-2 and iNOS protein levels

Protein levels of COX-2 and iNOS were further detected by western blot. Figure 6A and 6B shows that PRV induced obvious increases in the production of COX-2 and iNOS in RAW264.7 cells ($P<0.01$), showing a stimulus effect similar to that of LPS. Rutin or FEA treatment significantly decreased protein levels of COX-2 and iNOS in PRV-induced RAW264.7 cells, and 50 µg/ml FEA exhibited the strongest modulatory effect ($P<0.01$).

Effect of FEA on the phosphorylation of key proteins in the NF-κB and MAPK signaling pathways

Compared with those in the control cells, remarkably higher levels of IκBα phosphorylation and degradation were observed in the PRV-induced cells ($P<0.05$), while decreased phosphorylation and degradation of IκBα were observed in the virus-infected cells after rutin and FEA treatments. Among the tested drugs, 40 µg/ml rutin and 25 µg/ml FEA exhibited the strongest regulatory effects ($P<0.05$). In addition, phosphorylation of NF-κB p65 was significantly increased when RAW264.7 cells were infected with PRV or were treated with LPS ($P<0.01$), and this phosphorylation was remarkably inhibited by rutin or FEA treatment ($P<0.01$) (Fig. 6C and 6D). Phosphorylation of p38, ERK1/2, and JNK1/2, which are key proteins in the MAPK signaling pathway, was strongly increased in PRV-induced cells or in LPS-stimulated cells ($P<0.05$ or $P<0.01$) (Fig. 6E–H). However, the phosphorylation of these proteins was decreased by rutin and FEA treatment, leading to significantly lower levels of phosphorylated p38 and phosphorylated ERK compared to those observed after RPV incubation and LPS stimulation ($P<0.05$). The highest inhibitory effect on the phosphorylation of these two proteins was observed in cells treated with 50 µg/ml FEA. Although a lower level of phosphorylated JNK was observed in rutin or FEA-treated cells, the difference in the p-JNK/JNK ratio was not significant ($P>0.05$).

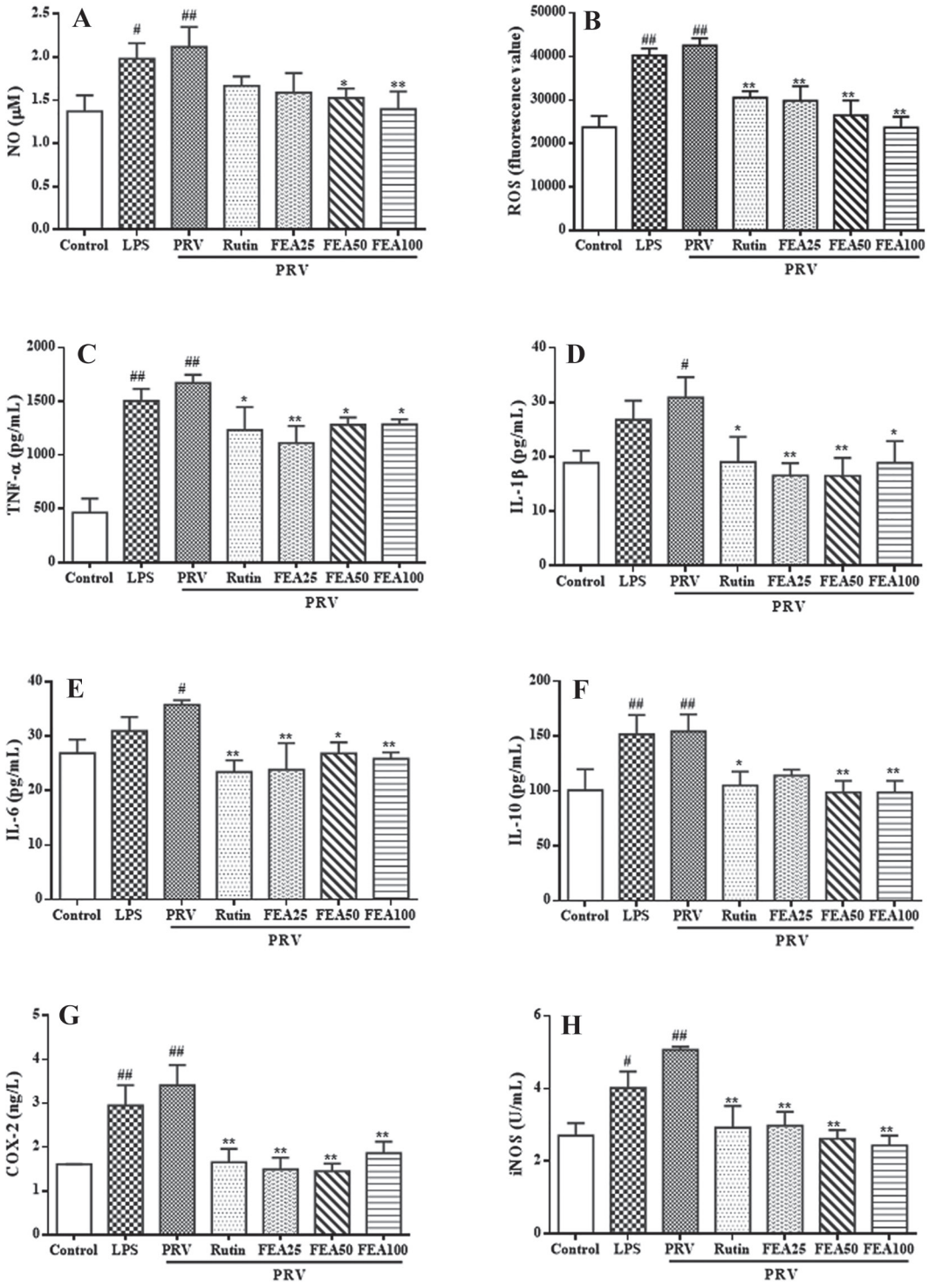

Fig. 4 Effects of ethyl acetate fraction of flavonoids from *Polygonum hydropiper L*. treatment on inflammatory factors. A: NO production was measured by No assay kit. B: reactive oxygen species (ROS) production was measured using a ROS Assay Kit. C-H: Secretion of tumor necrosis factor-α (TNF-α), interleukin-1β (IL-1β), interleukin-6 (IL-6), interleukin-10 (IL-10), and cyclooxygenase-2 (COX-2), and inducible nitric oxide synthase (iNOS) were measured by ELISA kits. The values are presented as mean ± S.D. # or ## means comparison between control group and all other groups (lipopolysaccharide (LPS) group, Pseudorabies virus (PRV) group, rutin group and ethyl acetate fraction of flavonoids (FEA) groups) (P<0.05, or P<0.01). * or ** only means comparison between PRV group and treatment groups (rutin group and FEA groups) (P<0.05, or P<0.01).

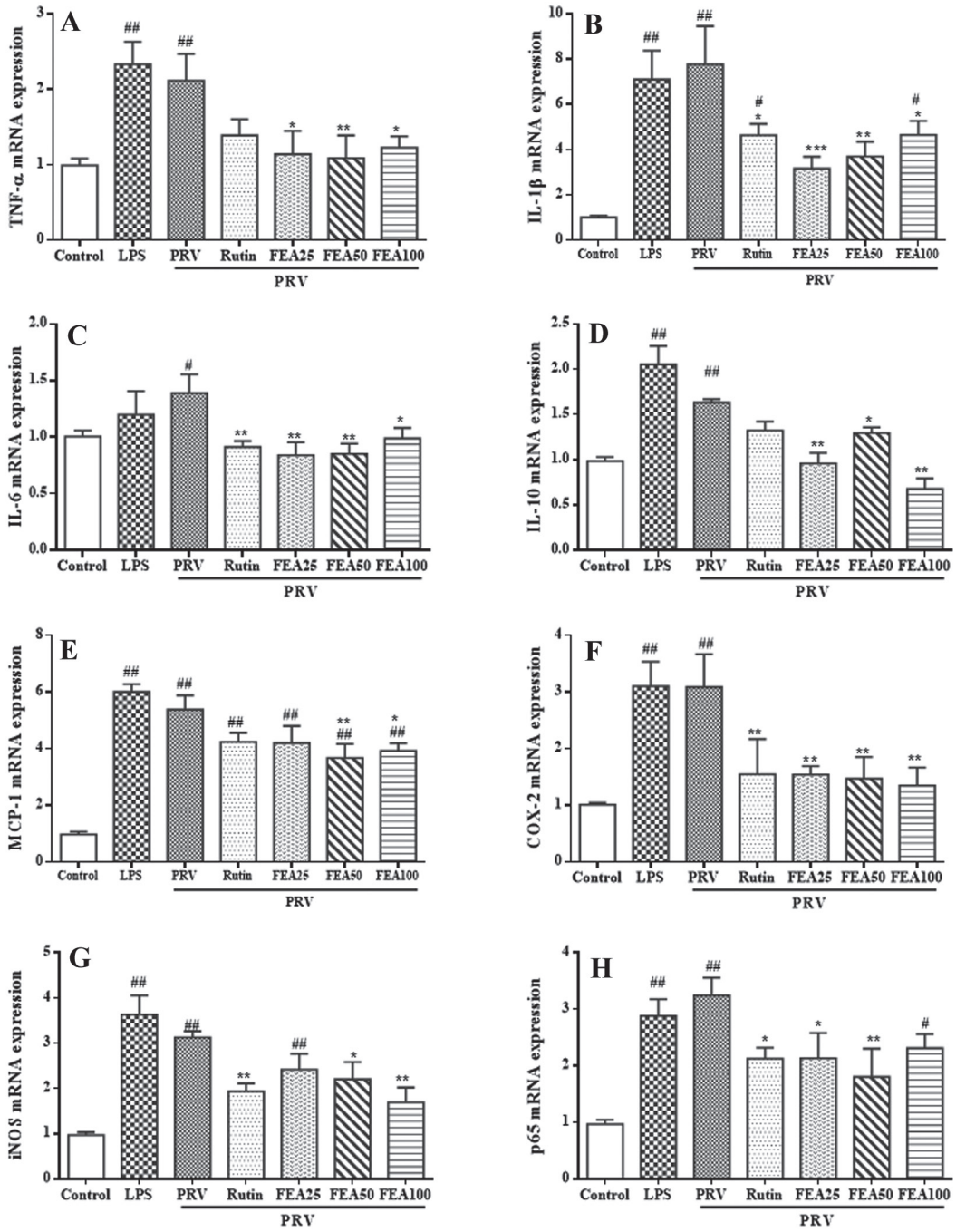

Fig. 5. Effects of ethyl acetate fraction of flavonoids from *Polygonum hydropiper L*. treatment on mRNA levels. Cells were exposed to Pseudorabies virus (PRV) or lipopolysaccharide (LPS) for 1.5 hr and then treated with or without ethyl acetate fraction of flavonoids (FEA) for another 8 hr. Relative mRNA levels of inflammatory biomarkers and nuclear factor-kappa B (NF-κB) p65 were detected by q-PCR. A: tumor necrosis factor-α (TNF-α), B: interleukin-1β (IL-1β), C: interleukin-6 (IL-6), D: interleukin-10 (IL-10), E: monocyte chemotactic protein-1 (MCP-1), F: cyclooxygenase-2 (COX-2), G: inducible nitric oxide synthase (iNOS), H: NF-κB p65. The values are presented as mean ± S.D. # or ## means comparison between control group and all the other groups (LPS group, PRV group, rutin group, and FEA groups) (P<0.05, or P<0.01). * or ** only means comparison between PRV group and treatment groups (rutin group and FEA groups) (P<0.05, or P<0.01).

DISCUSSION

The inflammatory response is a self-protective mechanism that occurs during pathogen infection or tissue injury that improves clearance of infected pathogens or injured cells [44]. However, uncontrolled inflammation leads to damage of normal cells and injury of the immune and nervous systems, which are phenomena commonly observed during viral infection and, in turn, leads to worsening of the disease [50]. PRV infection has caused severe central nervous system disorders in pigs or in mice by inducing

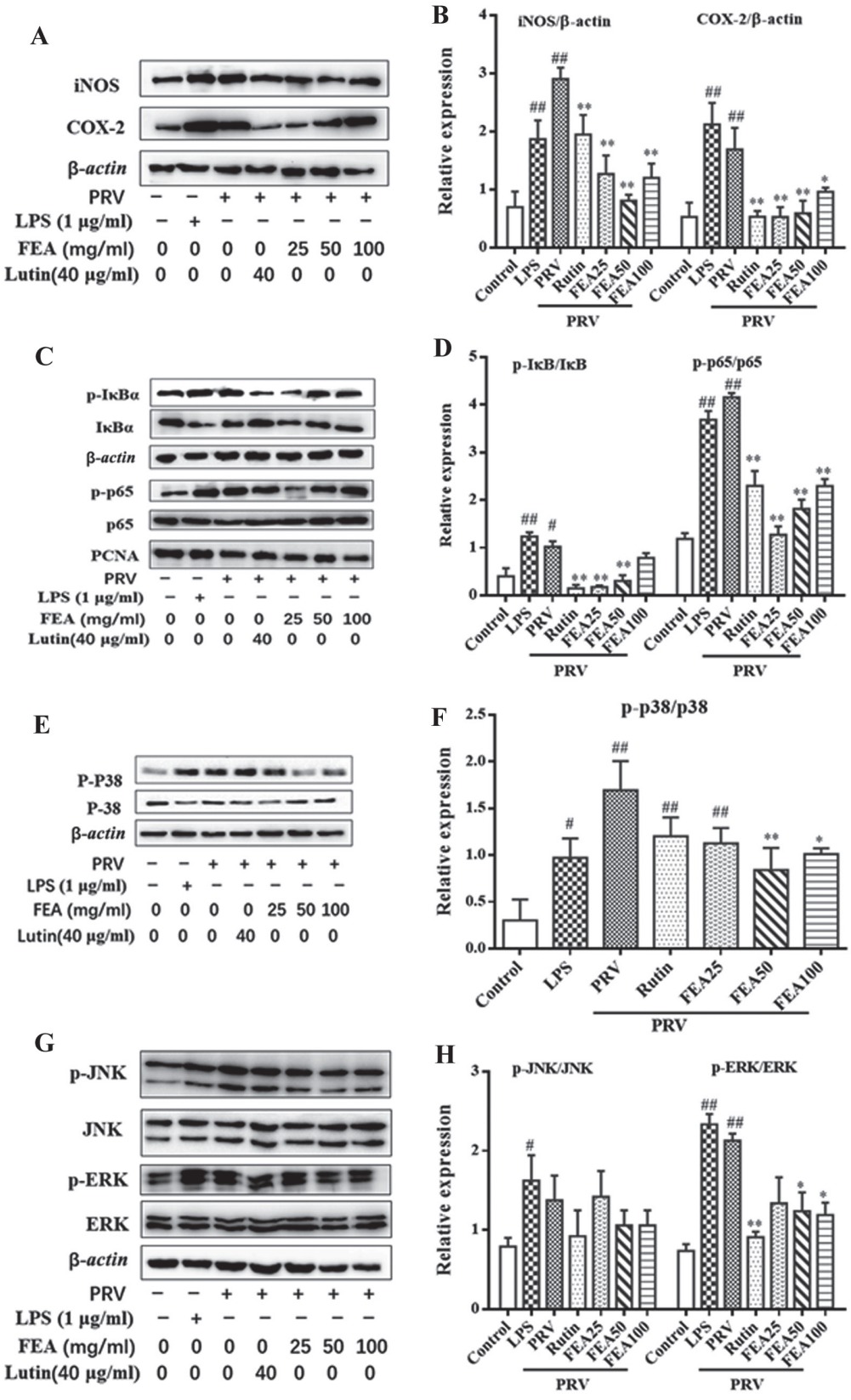

Fig. 6. Effects of ethyl acetate fraction of flavonoids from *Polygonum hydropiper L.* treatment on protein expression. Cells were exposed to Pseudorabies virus (PRV) or lipopolysaccharide (LPS) for 1.5 hr and then treated with or without ethyl acetate fraction of flavonoids (FEA) for another 8 hr. (A and B) Protein expression levels of cyclooxygenase-2 (COX-2) and inducible nitric oxide synthase (iNOS). (C and D) Protein expressions of p-p65/p65 and p-IκBα/IκBα. (E-H) Protein expressions of ERK1/2, JNK1/2, and p38 mitogen-activated protein kinase (MAPK). Values are presented as mean ± S.D. # or ## means comparison between control group and all other groups (LPS group, PRV group, rutin group, and FEA groups) (P<0.05, or P<0.01). * or ** only means comparison between PRV group and treatment groups (rutin group and FEA groups) (P<0.05, or P<0.01).

inflammation-mediated damage in the central nervous and immune organs [11, 22, 24, 32]. Thus, it is speculated that PRV-induced tissue damage and nervous disorders can be alleviated by modulating inflammatory response in the infected organism. Exogenous antioxidants such as plant extracts that contain large amounts of flavonoids have been reported to effectively control inflammatory response in PRV-induced immune cells and to reduce cell death and damage [27, 30]. RAW264.7 cells play important roles in the study of inflammatory response or in specific immune responses by producing pro-inflammatory cytokines and inflammatory mediators, thus, they have been widely used as cell models for the study of issues related to inflammation [8, 29, 40]. In this study, RAW264.7 cells were incubated with PRV to evaluate the protective effect of FAE against PRV-induced inflammatory damage and to elucidate the processes and mechanisms of viral infection.

P. hydropiper L. has been widely used to treat various diseases associated with inflammation such as intestinal inflammation and mouse ear inflammation [6, 49]. Flavonoids are the main secondary metabolites in *Polygonum* species, and previously identified flavonoids include rutin, hyperin, epicatechin, quercetin, quercitrin, kaempferol, isoquercitrin, and catechin. Among these flavonoids, rutin, quercetin, quercitrin, and kaempferol are the most abundant in *P. hydropiper L*. [46]. In our previous study, FNB extracted from *P. hydropiper L.* exhibited strong anti-oxidative and anti-inflammatory activities against LPS-induced oxidative stress [41]; however, whether FEA can regulate the excessive inflammatory response caused by viral infection has not yet been reported. In this study, FEA was extracted from *P. hydropiper L.,* the total flavonoid contents in the extract was quantitatively determined to be 56.8%, and the rutin, quercitrin, and quercetin contents in FEA were calculated to be 281.97 mg/g (28.20%), 160.98 mg/g (16.10%), and 83.31 mg/g (8.33%), respectively, accounting for a total of 52.63% of FEA, which is lower than the total flavonoid content due to the presence of other impurities. Thus, in this study, 50~60% of the main effective constituents in FEA may be necessary to perform the anti-inflammatory action by inhibiting the expression of inflammatory factors.

As safety is one of the most critical issues in the early stage of drug development, FEA cytotoxicity was first evaluated using RAW264.7 cells. No significant difference was observed in cell viability after RAW264.7 cells were cultured with FEA at concentrations ≤200 μg/ml, and it is worth noting that 50 and 100 μg/ml FEA slightly stimulated cell proliferation,providing a basis for screening the drug dose. Based on the above-mentioned HPLC analysis, 50~60% of the main effective constituents in FEA may be necessary to perform the anti-inflammatory action by inhibiting expression of inflammatory factors. The concentrations of active ingredients were consistent with previous reports stating that 15~30 μg/ml quercetin or rutin have antiviral activity [7].

High expressions of PRV mRNA were observed in PRV-induced cells, suggesting successful virus infection. Because LPS is an endotoxin often used to establish inflammatory models *in vitro* and *in vivo* to study inflammatory pathological changes and to identify anti-inflammatory drugs, LPS was used as a positive control in this study [16, 26]. Similar outcomes were observed in LPS-treated cells and in PRV-induced cells, such as decreased cell activity, increased NO and ROS levels, and enhanced release and expression of inflammatory cytokines compared to the control cells, indicating the occurrence of an inflammatory response in PRV-induced RAW264.7 cells. These results are consistent with our previous studies [40]. After PRV infection, FEA treatment induced a decrease in cell activity, NO and ROS production, and in the release and expression of inflammatory factors, indicating that FEA can modulate the PRV-induced inflammatory response. This is in accordance with a previous report stating that luteolin inhibits the viral-induced inflammatory response in RAW264.7 cells [30]. In our laboratory, we also investigated the anti-inflammatory activity of the FEA in porcine circovirus-infected porcine alveolar macrophages and found that FEA could attenuate porcine circovirus type 2 (PCV2)-induced inflammation in 3D4/2 cells, thereby fully demonstrating the anti-inflammatory activity of the FEA.

Activated macrophages are known to increase transcription levels of iNOS and COX-2 in response to a variety of inflammatory stimulants such as pro-inflammatory medium, viral infection, and LPS, whereas the up-regulated transcription of these genes leads to the overproduction of both NO and prostaglandin E2 (PGE2), thus leading to the exacerbation of inflammatory symptoms [21, 27]. Therefore, modulating the expression of iNOS and COX-2 is considered an effective therapeutic approach to decrease the side effects of immune activities and to prevent severe inflammatory disorders [9]. In the present study, FEA significantly inhibited PRV-induced iNOS and COX-2 expression, which was consistent with the increased cell viability and decreased inflammatory cytokine levels in the supernatant (Fig. 6A and 6B). Similar results were observed when PRV-infected RAW264.7 cells were treated with the *Dunaliella salina* (*D. salina*) carotenoid extract [28, 30].

NF-κB is critical in regulating inflammatory responses by activating transcription and expression of inflammatory mediators and pro-inflammatory cytokines [17, 33, 34]. Normally, NF-κB p65 is retained in the cytoplasm by tightly binding to IκBα. When the NF-κB signaling pathway is activated by stimulants such as LPS or viral infections, IκB is phosphorylated and undergoes ubiquitin- mediated degradation, leading to the release and translocation of phosphorylated NF-κB p65 into the nucleus. Phosphorylated NF-κB p65 in the nucleus eventually activates transcription and expression of genes associated with inflammation such as iNOS and COX-2 [38, 42, 45]. In this study, phosphorylation and degradation of IκBα were significantly inhibited by treatment with FEA, leading to the cytoplasmic retention of NF-κB p65 and decreased levels of NF-κB p65 in the nuclear fraction of PRV-induced RAW264.7 cells. This decreased translocation of NF-κB p65 into the nucleus may account for the decrease in transcription and production of inflammatory cytokines such as TNF-α, IL-1β, IL-6, IL-10, COX-2, and iNOS. These observations are consistent with literature stating that berberine and algae modulate the inflammatory response induced by viruses by inhibiting activation of the NF-κB signaling pathway [3, 29].

MAPKs, including ERK1/2, JNK1/2, and p38 MAPK, are important kinases in the MAPK signaling pathways that are also critical in regulating inflammatory mediator production and cell survival in macrophages [12, 36]. Previous studies have shown that MAPKs activated by LPS or PRV are involved in the increased expression of iNOS, COX-2, and pro-inflammatory cytokines, while such activation could be attenuated by β-carotene or algae [3, 27]. In this study, phosphorylation of ERK1/2 and p38 MAPK

was significantly increased upon LPS stimulation or PRV infection, whereas phosphorylation of these important kinases was inhibited by FEA treatment, suggesting that anti-inflammatory activities of FEA may be partially due to the inhibition of the MAPK signaling pathways.

In conclusion, a cell model of inflammation was established through PRV infection, which showed outcomes similar to those created through LPS stimulation, such as decreased cell viability, increased NO and ROS production, enhanced pro-inflammatory cytokine release, and up-regulated gene expression. Thus, FEA treatment attenuated PRV-induced inflammation by inhibiting activation of the NF-κB and MAPK pathways.

CONFLICT OF INTEREST. There were no conflicts of interest on any front.

ACKNOWLEDGMENTS. We thank Dr. Huang Weijian of the Laboratory of Animal Infectious Disease in the College of Animal Science and Technology, Guangxi University for his kindness in providing PRV. This work was financially supported by the National Natural Science Fund of China (Grant number: 32072907), the Innovation Driven Development Fund of Guangxi (Grant number: AA17204081-2), and the Guangxi Innovation Team Building Project of the National Modern Agricultural Industry Technology System (Grant number: nycytxgxcxtd-14-02).

REFERENCES

1. Abd El-Kader, A. M., El-Readi, M. Z., Ahmed, A. S., Nafady, A. M., Wink, M. and Ibraheim, Z. Z. 2013. Polyphenols from aerial parts of Polygonum bellardii and their biological activities. *Pharm. Biol.* **51**: 1026–1034. [Medline] [CrossRef]
2. Adnan, A., Allaudin, Z. N., Hani, H., Loh, H. S., Khoo, T. J., Ting, K. N. and Abdullah, R. 2019. Virucidal activity of Garcinia parvifolia leaf extracts in animal cell culture. *BMC Complement. Altern. Med.* **19**: 169. [Medline] [CrossRef]
3. Amasheh, M., Fromm, A., Krug, S. M., Amasheh, S., Andres, S., Zeitz, M., Fromm, M. and Schulzke, J. D. 2010. TNFalpha-induced and berberine-antagonized tight junction barrier impairment via tyrosine kinase, Akt and NFkappaB signaling. *J. Cell Sci.* **123**: 4145–4155. [Medline] [CrossRef]
4. An, T. Q., Peng, J. M., Tian, Z. J., Zhao, H. Y., Li, N., Liu, Y. M., Chen, J. Z., Leng, C. L., Sun, Y., Chang, D. and Tong, G. Z. 2013. Pseudorabies virus variant in Bartha-K61-vaccinated pigs, China, 2012. *Emerg. Infect. Dis.* **19**: 1749–1755. [Medline] [CrossRef]
5. Ayaz, M., Junaid, M., Ahmed, J., Ullah, F., Sadiq, A., Ahmad, S. and Imran, M. 2014. Phenolic contents, antioxidant and anticholinesterase potentials of crude extract, subsequent fractions and crude saponins from Polygonum hydropiper L. *BMC Complement. Altern. Med.* **14**: 145. [Medline] [CrossRef]
6. Bralley, E. E., Greenspan, P., Hargrove, J. L., Wicker, L. and Hartle, D. K. 2008. Topical anti-inflammatory activity of Polygonum cuspidatum extract in the TPA model of mouse ear inflammation. *J. Inflamm. (Lond.)* **5**: 1. [Medline] [CrossRef]
7. Carvalho, O. V., Botelho, C. V., Ferreira, C. G. T., Ferreira, H. C. C., Santos, M. R., Diaz, M. A., Oliveira, T. T., Soares-Martins, J. A., Almeida, M. R. and Silva, A. Jr. 2013. In vitro inhibition of canine distemper virus by flavonoids and phenolic acids: implications of structural differences for antiviral design. *Res. Vet. Sci.* **95**: 717–724. [Medline] [CrossRef]
8. Chen, H. L., Tan, H. L., Yang, J., Wei, Y. Y. and Hu, T. J. 2018. Sargassum polysaccharide inhibits inflammatory response in PCV2 infected-RAW264.7 cells by regulating histone acetylation. *Carbohydr. Polym.* **200**: 633–640. [Medline] [CrossRef]
9. Chen, N., Warner, J. L. and Reiss, C. S. 2000. NSAID treatment suppresses VSV propagation in mouse CNS. *Virology* **276**: 44–51. [Medline] [CrossRef]
10. Chen, Y. M., Huang, C. C., Hsiao, C. Y., Hu, S., Wang, I. L. and Sung, H. C. 2019. Ludwigia octovalvis (Jacq.) raven extract supplementation enhances muscle glycogen content and endurance exercise performance in mice. *J. Vet. Med. Sci.* **81**: 667–674. [Medline] [CrossRef]
11. Cong, X., Lei, J. L., Xia, S. L., Wang, Y. M., Li, Y., Li, S., Luo, Y., Sun, Y. and Qiu, H. J. 2016. Pathogenicity and immunogenicity of a gE/gI/TK gene-deleted pseudorabies virus variant in susceptible animals. *Vet. Microbiol.* **182**: 170–177. [Medline] [CrossRef]
12. Coskun, M., Olsen, J., Seidelin, J. B. and Nielsen, O. H. 2011. MAP kinases in inflammatory bowel disease. *Clin. Chim. Acta* **412**: 513–520. [Medline] [CrossRef]
13. Devarajan, S., Yahiro, E., Uehara, Y., Kuroda, R., Hirano, Y., Nagata, K., Miura, S., Saku, K. and Urata, H. 2018. Depressor effect of the young leaves of Polygonum hydropiper Linn. in high-salt induced hypertensive mice. *Biomed. Pharmacother.* **102**: 1182–1187. [Medline] [CrossRef]
14. Fan, D., Zhou, X., Zhao, C., Chen, H., Zhao, Y. and Gong, X. 2011. Anti-inflammatory, antiviral and quantitative study of quercetin-3-O-β-D-glucuronide in Polygonum perfoliatum L. *Fitoterapia* **82**: 805–810. [Medline] [CrossRef]
15. Freuling, C. M., Müller, T. F. and Mettenleiter, T. C. 2017. Vaccines against pseudorabies virus (PrV). *Vet. Microbiol.* **206**: 3–9. [Medline] [CrossRef]
16. Geraets, L., Haegens, A., Brauers, K., Haydock, J. A., Vernooy, J. H. J., Wouters, E. F. M., Bast, A. and Hageman, G. J. 2009. Inhibition of LPS-induced pulmonary inflammation by specific flavonoids. *Biochem. Biophys. Res. Commun.* **382**: 598–603. [Medline] [CrossRef]
17. Gilmore, T. D. 2006. Introduction to NF-kappaB: players, pathways, perspectives. *Oncogene* **25**: 6680–6684. [Medline] [CrossRef]
18. Gonçalves, J. L., Leitão, S. G., Monache, F. D., Miranda, M. M., Santos, M. G., Romanos, M. T. and Wigg, M. D. 2001. In vitro antiviral effect of flavonoid-rich extracts of Vitex polygama (Verbenaceae) against acyclovir-resistant herpes simplex virus type 1. *Phytomedicine* **8**: 477–480. [Medline] [CrossRef]
19. Gu, Z., Hou, C., Sun, H., Yang, W., Dong, J., Bai, J. and Jiang, P. 2015. Emergence of highly virulent pseudorabies virus in southern China. *Can. J. Vet. Res.* **79**: 221–228. [Medline]
20. Jing, L., Ma, H., Fan, P., Gao, R. and Jia, Z. 2015. Antioxidant potential, total phenolic and total flavonoid contents of Rhododendron anthopogonoides and its protective effect on hypoxia-induced injury in PC12 cells. *BMC Complement. Altern. Med.* **15**: 287. [Medline] [CrossRef]
21. Kubes, P. and McCafferty, D. M. 2000. Nitric oxide and intestinal inflammation. *Am. J. Med.* **109**: 150–158. [Medline] [CrossRef]
22. Lai, I. H., Chang, C. D. and Shih, W. L. 2019. Apoptosis induction by pseudorabies virus via oxidative stress and subsequent DNA damage signaling. *Intervirology* **62**: 116–123. [Medline] [CrossRef]
23. Lani, R., Hassandarvish, P., Shu, M. H., Phoon, W. H., Chu, J. J., Higgs, S., Vanlandingham, D., Abu Bakar, S. and Zandi, K. 2016. Antiviral activity of selected flavonoids against Chikungunya virus. *Antiviral Res.* **133**: 50–61. [Medline] [CrossRef]
24. Lee, H., Sunden, Y., Ochiai, K. and Umemura, T. 2011. Experimental intracerebral vaccination protects mouse from a neurotropic virus by attracting

antibody secreting cells to the CNS. *Immunol. Lett.* **139**: 102–109. [Medline] [CrossRef]
25. Lerma, L., Muñoz, A. L., Wagner, S., Dinu, M., Martín, B. and Tabarés, E. 2016. Construction of recombinant pseudorabies viruses by using PRV BACs deficient in IE180 or pac sequences: application of vBAC90D recombinant virus to production of PRV amplicons. *Virus Res.* **213**: 274–282. [Medline] [CrossRef]
26. Li, H., Yoon, J. H., Won, H. J., Ji, H. S., Yuk, H. J., Park, K. H., Park, H. Y. and Jeong, T. S. 2017. Isotrifoliol inhibits pro-inflammatory mediators by suppression of TLR/NF-κB and TLR/MAPK signaling in LPS-induced RAW264.7 cells. *Int. Immunopharmacol.* **45**: 110–119. [Medline] [CrossRef]
27. Lin, H. W., Chang, T. J., Yang, D. J., Chen, Y. C., Wang, M. and Chang, Y. Y. 2012. Regulation of virus-induced inflammatory response by β-carotene in RAW264.7 cells. *Food Chem.* **134**: 2169–2175. [Medline] [CrossRef]
28. Lin, H. W., Chen, Y. C., Liu, C. W., Yang, D. J., Chen, S. Y., Chang, T. J. and Chang, Y. Y. 2014. Regulation of virus-induced inflammatory response by Dunaliella salina alga extract in macrophages. *Food Chem. Toxicol.* **71**: 159–165. [Medline] [CrossRef]
29. Lin, H. W., Liu, C. W., Yang, D. J., Chen, C. C., Chen, S. Y., Tseng, J. K., Chang, T. J. and Chang, Y. Y. 2017. Dunaliella salina alga extract inhibits the production of interleukin-6, nitric oxide, and reactive oxygen species by regulating nuclear factor-κB/Janus kinase/signal transducer and activator of transcription in virus-infected RAW264.7 cells. *Yao Wu Shi Pin Fen Xi* **25**: 908–918. [Medline]
30. Liu, C. W., Lin, H. W., Yang, D. J., Chen, S. Y., Tseng, J. K., Chang, T. J. and Chang, Y. Y. 2016. Luteolin inhibits viral-induced inflammatory response in RAW264.7 cells via suppression of STAT1/3 dependent NF-κB and activation of HO-1. *Free Radic. Biol. Med.* **95**: 180–189. [Medline] [CrossRef]
31. Machado, V. B., Maróstica de Sá, J., Miranda Prado, A. K., Alves de Toledo, K., Regasini, L. O., Pereira de Souza, F., Caruso, I. P. and Fossey, M. A. 2019. Biophysical and flavonoid-binding studies of the G protein ectodomain of group A human respiratory syncytial virus. *Heliyon* **5**: e01394. [Medline] [CrossRef]
32. Maqbool, B., Wang, Y., Cui, X., He, S., Guan, R., Wang, S., Wang, Y. and Hu, S. 2019. Ginseng stem-leaf saponins in combination with selenium enhance immune responses to an attenuated pseudorabies virus vaccine. *Microbiol. Immunol.* **63**: 269–279. [Medline] [CrossRef]
33. Nakamura, T., Suzuki, H., Wada, Y., Kodama, T. and Doi, T. 2006. Fucoidan induces nitric oxide production via p38 mitogen-activated protein kinase and NF-kappaB-dependent signaling pathways through macrophage scavenger receptors. *Biochem. Biophys. Res. Commun.* **343**: 286–294. [Medline] [CrossRef]
34. Perkins, N. D. 2007. Integrating cell-signalling pathways with NF-kappaB and IKK function. *Nat. Rev. Mol. Cell Biol.* **8**: 49–62. [Medline] [CrossRef]
35. Poeck, H. and Ruland, J. 2012. From virus to inflammation: mechanisms of RIG-I-induced IL-1β production. *Eur. J. Cell Biol.* **91**: 59–64. [Medline] [CrossRef]
36. Pontes, M. S., Van Waesberghe, C., Nauwynck, H., Verhasselt, B. and Favoreel, H. W. 2016. Pseudorabies virus glycoprotein gE triggers ERK1/2 phosphorylation and degradation of the pro-apoptotic protein Bim in epithelial cells. *Virus Res.* **213**: 214–218. [Medline] [CrossRef]
37. Rahman, E., Goni, S. A., Rahman, M. T. and Ahmed, M. 2002. Antinociceptive activity of Polygonum hydropiper. *Fitoterapia* **73**: 704–706. [Medline] [CrossRef]
38. Ren, D., Lin, D., Alim, A., Zheng, Q. and Yang, X. 2017. Chemical characterization of a novel polysaccharide ASKP-1 from Artemisia sphaerocephala Krasch seed and its macrophage activation via MAPK, PI3k/Akt and NF-κB signaling pathways in RAW264.7 cells. *Food Funct.* **8**: 1299–1312. [Medline] [CrossRef]
39. Shi, X., Liu, D., Zhang, J., Hu, P., Shen, W., Fan, B., Ma, Q. and Wang, X. 2016. Extraction and purification of total flavonoids from pine needles of Cedrus deodara contribute to anti-tumor in vitro. *BMC Complement. Altern. Med.* **16**: 245. [Medline] [CrossRef]
40. Su, Z. J., Wei, Y. Y., Yin, D., Shuai, X. H., Zeng, Y. and Hu, T. J. 2013. Effect of Sophora subprosrate polysaccharide on oxidative stress induced by PCV2 infection in RAW264.7 cells. *Int. J. Biol. Macromol.* **62**: 457–464. [Medline] [CrossRef]
41. Tao, J., Wei, Y. and Hu, T. 2016. Flavonoids of Polygonum hydropiper L. attenuates lipopolysaccharide-induced inflammatory injury via suppressing phosphorylation in MAPKs pathways. *BMC Complement. Altern. Med.* **16**: 25. [Medline] [CrossRef]
42. Viatour, P., Merville, M. P., Bours, V. and Chariot, A. 2005. Phosphorylation of NF-kappaB and IkappaB proteins: implications in cancer and inflammation. *Trends Biochem. Sci.* **30**: 43–52. [Medline] [CrossRef]
43. Wang, Y., Qiao, S., Li, X., Xie, W., Guo, J., Li, Q., Liu, X., Hou, J., Xu, Y., Wang, L., Guo, C. and Zhang, G. 2015. Molecular epidemiology of outbreak-associated pseudorabies virus (PRV) strains in central China. *Virus Genes* **50**: 401–409. [Medline] [CrossRef]
44. Weitz-Schmidt, G. 2002. Statins as anti-inflammatory agents. *Trends Pharmacol. Sci.* **23**: 482–486. [Medline] [CrossRef]
45. Yang, D. J., Chang, Y. Y., Lin, H. W., Chen, Y. C., Hsu, S. H. and Lin, J. T. 2014. Inhibitory effect of litchi (Litchi chinensis Sonn.) flower on lipopolysaccharide-induced expression of proinflammatory mediators in RAW264.7 cells through NF-κB, ERK, and JAK2/STAT3 inactivation. *J. Agric. Food Chem.* **62**: 3458–3465. [Medline] [CrossRef]
46. Yang, X., Wang, B. C., Zhang, X., Yang, S. P., Li, W., Tang, Q. and Singh, G. K. 2011. Simultaneous determination of nine flavonoids in Polygonum hydropiper L. samples using nanomagnetic powder three-phase hollow fibre-based liquid-phase microextraction combined with ultrahigh performance liquid chromatography-mass spectrometry. *J. Pharm. Biomed. Anal.* **54**: 311–316. [Medline] [CrossRef]
47. Yang, Y., Yu, T., Jang, H. J., Byeon, S. E., Song, S. Y., Lee, B. H., Rhee, M. H., Kim, T. W., Lee, J., Hong, S. and Cho, J. Y. 2012. In vitro and in vivo anti-inflammatory activities of Polygonum hydropiper methanol extract. *J. Ethnopharmacol.* **139**: 616–625. [Medline] [CrossRef]
48. Ye, C., Zhang, Q. Z., Tian, Z. J., Zheng, H., Zhao, K., Liu, F., Guo, J. C., Tong, W., Jiang, C. G., Wang, S. J., Shi, M., Chang, X. B., Jiang, Y. F., Peng, J. M., Zhou, Y. J., Tang, Y. D., Sun, M. X., Cai, X. H., An, T. Q. and Tong, G. Z. 2015. Genomic characterization of emergent pseudorabies virus in China reveals marked sequence divergence: Evidence for the existence of two major genotypes. *Virology* **483**: 32–43. [Medline] [CrossRef]
49. Zhang, W., Pan, Y., Qu, S., Wang, D., Cheng, S. and Liu, X. 2018. Anti-inflammatory effects of an extract of *Polygonum hydropiper* stalks on 2,4,6-trinitrobenzenesulphonic acid-induced intestinal inflammation in rats by inhibiting the NF-κB pathway. *Mediators Inflamm.* **2018**: 6029135. [Medline] [CrossRef]
50. Zhang, X., Shu, X., Bai, H., Li, W., Li, X., Wu, C., Gao, Y., Wang, Y., Yang, K. and Song, C. 2019. Effect of porcine circovirus type 2 on the severity of lung and brain damage in piglets infected with porcine pseudorabies virus. *Vet. Microbiol.* **237**: 108394. [Medline] [CrossRef]
51. Zouharova, D., Lipenska, I., Fojtikova, M., Kulich, P., Neca, J., Slany, M., Kovarcik, K., Turanek-Knotigova, P., Hubatka, F., Celechovska, H., Masek, J., Koudelka, S., Prochazka, L., Eyer, L., Plockova, J., Bartheldyova, E., Miller, A. D., Ruzek, D., Raska, M., Janeba, Z. and Turanek, J. 2016. Antiviral activities of 2,6-diaminopurine-based acyclic nucleoside phosphonates against herpesviruses: In vitro study results with pseudorabies virus (PrV, SuHV-1). *Vet. Microbiol.* **184**: 84–93. [Medline] [CrossRef]